Journal of Materials Chemistry A

ARTICLE

Highly Mesoporous Carbons Derived from Biomass Feedstocks Templated with Eutectic Salt ZnCl2/KCl

Zhishuang Ma, Hongye Zhang, Zhenzhen Yang, Yanfei Zhang, Bo Yu, Zhimin Liu*

Highly mesoporous carbons (MCs) were prepared by carbonization of biomass sources including glucose, cellulose and lignin, with eutectic salt (KCl/ZnCl2, denoted as PZ) as the porogen agent and catalyst. The influences of the mass ratio of carbon sources to PZ, heating program, calcination temperature on the textural structures of the carbons were investigated. It was demonstrated that the MC derived from glucose with a mass ratio of glucose to PZ at 1: 6 exhibited a specific surface area (SSA) of 1297 $m^2 \cdot g^{-1}$ and pore volume of 2.727 $cm^3 \cdot g^{-1}$ dominated with mesopore volume proportion of 92.2%, and the MCs from cellulose and lignin also showed relatively high mesoporous proportions in the range of 63.2%-87.5% and SSAs higher than 1000 $m^2 \cdot g^{-1}$. Furthermore, based on the TGA, FT-IR and N_2 sorption analyses, the generation of high proportion of mesopores in MCs was discussed.

Introduction

Mesoporous carbon (MC, i.e., carbon with pores of intermediate size, 2-50 nm) has attracted more and more attention owning to its unique properties such as extraordinary chemical, mechanical and thermal stability and wide abundance in nature.[1] Nowadays, the widespread applications of MCs in areas such as supercapacitors, chemical sensors, catalyst supports, fuel cells and separation sorbents have encouraged the researchers to synthesize porous carbons with high mesoporous volume proportion and high specific surface area (SSA).[2-7] Therefore, it is important to develop reliable methods for the preparation of MCs with controllable porosity, together with high SSA and large pore volume.

In the past decades, numerous carbon resources, such as fossil based hydrocarbons (e.g., bituminous coal, lignite), biomass (e.g., glucose, cellulose, lignin and wood), polymers etc., have been utilized for the preparation of MCs. Especially, biomass including cellulose, lignin and their platform molecules provides abundant feedstock for the preparation of carbon materials.[8-22] Due to the presence of plentiful oxygen in the biomass resource, the carbons derived from the biomass generally contain oxygen-containing groups, which may provide the carbons specific functions. Thus, preparation of porous carbons from biomass has been paid much attention.

For the preparation of porous carbon materials, the porogens such as surfactants,[9, 23, 24] salts[25-29] and their mixtures[30, 31] are generally required. Zinc chloride ($ZnCl_2$) is one of the porogens widely used in the preparation of activated carbon (AC) from biomass (e.g., olive stones, oil palm shells and Kraft lignin), which can result in porous carbon materials with high SSAs

(e.g., 800-2170 $m^2 \cdot g^{-1}$) and high carbon yields.[15, 32-36] However, the proportions of mesopore in the resultant ACs are generally low (5-40%).[9, 23, 32, 37] Recently, Antonietti and co-workers utilized eutectic salt composing of $ZnCl_2$ and chloride salts as the porogen to regulate the pore diameters of the carbon materials derived from ionic liquids.[30] The combination of $ZnCl_2$ with different salts could tune the pore size of the resultant carbons. For example, $LiCl/ZnCl_2$ resulted in microporous carbons; $NaCl/ZnCl_2$ afforded microporous and small mesoporous carbons, while $KCl/ZnCl_2$ mainly resulted in MCs with large mesopores. The $ZnCl_2$-based eutectic salt showed promising potentials for the preparation of MCs. However, it was seldom applied in the preparation of MCs from biomass carbonization.[31, 38-40]

In this work, biomass including glucose, cellulose and lignin was used as the carbon resources, and the $KCl/ZnCl_2$ mixture with the molar ratio of $KCl: ZnCl_2$ at 51: 49 (denoted as PZ, melting point at 230 °C)[30] as the porogen agent for the preparation of MCs. The porogen, PZ, mixed directly with the carbon resource via grinding, followed by calcination with a gradient or linear temperature program, resulting in porous carbons after the removal of the porogen salts. A series of porous carbons were obtained via changing carbon resources (e.g., glucose, cellulose and lignin), the weight ratio of carbon resource to the porogen, heating program, and the final calcination temperature. The resultant samples were examined by means of different techniques including TGA, FT-IR, scanning electron microscopy (SEM), transmission electron microscopy (TEM), N_2 sorption and X-ray diffraction (XRD).

In addition, the possible formation mechanism of the MCs was discussed.

Experimental section

Materials

Glucose, microcrystalline cellulose, and lignin were purchased from Alfa Aesar. KCl and $ZnCl_2$ (99%) were acquired from Sinopharm Chemical Reagent. All chemicals were used without further purification.

Procedures for preparation of MCs

Glucose, microcrystalline cellulose and lignin were used as carbon resources, respectively. The mixture of KCl and $ZnCl_2$ with 51 mol% KCl was first prepared by grinding, used as the porogen for MC preparation.[30] In a typical experiment to prepare MC using glucose as the carbon resource, glucose (3.0 g) was mixed with PZ (9.0 g) by grinding at room temperature. Subsequently, the mixture was transferred into a ceramic boat, and moved to a tubular furnace for carbonization under nitrogen atmosphere with a flow rate of 100 mL/min. Two heating modes were adopted: linear temperature program (L) and gradient temperature program (G). In the former, the sample was heated with a heating rate of 1 °C/min from room temperature to the final temperature (e.g., 1000 °C), and kept at the final temperature for 2 h. In the latter, the temperature was increased from ambient temperature to 240 °C with a heating rate of 3 °C/min and held at this temperature for 2 h; then the temperature was further increased to the final calcination temperature (e.g., 400, 1000 °C) with a heating rate of 1 °C/min, and maintained at the final temperature for 2 h. Afterwards, the tubular furnace was allowed to cool down to room temperature under nitrogen atmosphere. The resultant mixture was ground into powder in an agate mortar, and washed with sufficient deionized water at room temperature to remove the salts until there was no Cl$^-$ detected in the supernatant. The resultant sample was dried under vacuum at 60 °C for 12 h. Different samples using glucose as the carbon resource were obtained via changing the mass ratio of glucose to PZ, heating mode and the final calcination temperature.

Similarly, using microcrystalline cellulose and lignin as the carbon resources, respectively, various MC samples were prepared using the above procedures. The obtained samples were denoted as A (G, C, L)-PZ (or Z)-T-Y (G, L), where A stands for carbon resource (G for glucose, C for cellulose and L for lignin), PZ for the eutectic salt composed of 51% KCl (P) and 49% $ZnCl_2$ (Z), T for the final calcination temperature and Y for the heating program (G for gradient temperature program, and L for linear temperature program).

Characterization

XRD analysis was performed on a Rigaku D/MAX-2500 diffraction using Ni-filtered Cu Kα radiation (λ = 1.5418 Å), in range of 3-80° (2θ) with a step width of 0.02°. The morphology of the sample was observed by field emission SEM on a scanning electron microscope (S-4800, Hitachi, Japan) and by TEM on a transmission electron microscope (JEM1011, JEOL, Japan) equipped with energy dispersive spectroscopy (EDS). The SSA and pore structure were investigated with a Quantachrome Quadrasorb SI-MP porosimeter using nitrogen as the adsorbate at 77 K. Prior to determination of the isotherm, the samples were degassed at 300 °C under vacuum for at least 3 h. The value of the total pore volume (V_{total}) was determined from the NLDFT kernel at the relative pressure P/P$_0$ = 0.99. The micropore volume (V_{micro}) was estimated using the α_s method.[41] The mesopore volume was calculated by subtraction of micropore volume from the total pore volume ($V_{meso} = V_{total} - V_{micro}$). The total SSA ($S_{total}$) was calculated using the Brunauer-Emmett-Teller (BET) method from the nitrogen adsorption data in the relative pressure (P/P$_0$) of 0.03-0.30. TGA analysis was carried out with a Perkin Elmer thermoanalyzer (model: Diamond TG/DTA). The weight loss was recorded in the range of 40-1000 °C. Each run consisted of the following steps: about 10 mg of sample was heated from 40 to 1000 °C at a ramping rate 10 °C/min under nitrogen atmosphere with the flow rate of 200 mL/min. FT-IR analyses of the samples were performed using a Bruker Optic TENSOR-37. All samples were mixed with KBr and determined in the range of 4000-400 cm^{-1} wavenumbers.

Results and discussion

In this work, various carbon samples were prepared via changing carbon resources (e.g., glucose, cellulose and lignin), porogen agent, mass ratio of carbon resource to porogen, heating mode, and final calcination temperature. To explore a suitable heating mode for the preparation of MCs using glucose as the carbon resource, the TGA analysis for glucose, PZ and the mixture of glucose and PZ with the mass ratio of 1: 3 were carried out, and the TGA curves are shown in Figure 1. From the TGA plot of pristine glucose, it was clear that the weight loss of glucose started at 200 °C, and dramatically increased up to 80% at 400 °C, implying that the carbonization of glucose mainly occurred in the temperature range of 200-400 °C. Further increasing temperature to 1000 °C, the weight loss increased slowly until around 10% was remained. In the TGA plot of PZ, the weight loss started at 500 °C, probably ascribing to the evaporation of the salts. As for the TGA plot of the glucose/PZ mixture, two obvious weight losses appeared. The sharp weight loss in the temperature range of 150-250 °C may be ascribed to the carbonization of glucose, while the other weight loss may be due to the further carbonization of the carbon from glucose and the evaporation of PZ. It is worthy noticing that the conversion of glucose started at 150°C in the presence of PZ, much lower than the decomposition temperature of glucose, implying that PZ catalyzed the conversion of glucose. Based on the TGA results and considering that PZ was in liquid state at 240°C and could catalyze the glucose conversion, two heating modes as described in the experimental sections were chosen for the preparation of carbon materials in this work.
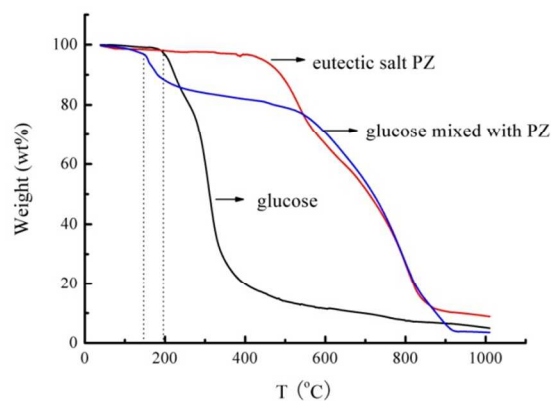
Figure 1 TGA results of glucose, eutectic salt PZ and glucose mixed with PZ mixture (1/3 ratio).
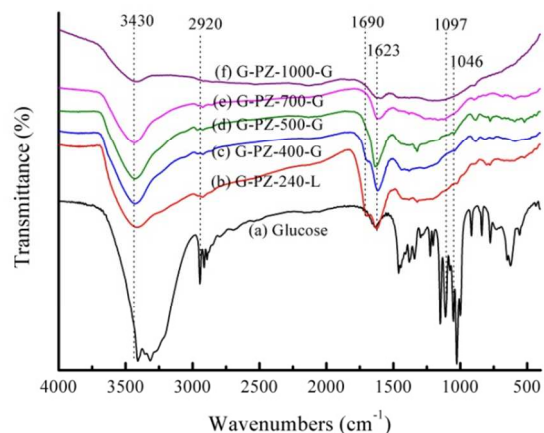

Figure 2 FT-IR spectrums of glucose and resultant MC samples.

The samples prepared using glucose as the carbon resource at different calcination temperatures were examined by FT-IR, and the FT-IR spectrums are shown in Figure 2. Compared to the spectrum of pristine glucose, the spectrum of each resultant sample shows declined corresponding peaks, accompanied with the appearance of new bands around 1623 and 1690 cm^{-1}. In the spectrum of sample G-PZ-240-L which was prepared at calcination temperature of 240 °C, the bands around 3430 cm^{-1} were assigned to the stretching vibration of the O-H bond, and those around 2920 cm^{-1} and 1046 cm^{-1} were corresponded to C-H vibrations. These bands became wider and less intense compared to those of glucose, suggesting that most of O-H and C-H bonds from glucose were disappeared in this sample. Moreover, the band at 1097 cm^{-1} in the FT-IR spectrum of glucose corresponding to C-O bond vibration almost disappeared in the spectrum of sample G-PZ-240-L, indicating the cleavage of C-O bond from glucose molecule. Notably, the new bands appearing at 1623 and 1690 cm^{-1} in the spectrum of G-PZ-240-L were corresponded to C=C and C=O vibrations, respectively. This indicated that glucose was converted to C=O containing compounds catalyzed by PZ,[19, 20, 41] identical to the TGA results. The other samples, G-PZ-400-G to G-PZ-1000-G, were prepared via further calcining G-PZ-240-L from 240 °C to the final calcination temperature with a heating rate of 1 °C/min, and kept at the corresponding final temperature for 2 h. From the FT-IR spectra of these samples, it was clear that the bands around 3430 and 2920 cm^{-1} gradually became weaker and weaker until almost disappeared as the calcination temperature increased. Especially, there hardly appeared any band in the IR spectrum of sample G-PZ-1000-G, suggesting that most oxygen-containing bonds from the carbon resource were damaged in the carbonization process. In this work, 1000 °C was selected as the final calcination temperature for preparing MC materials.

The morphology and structure of the samples prepared at the calcination temperature of 1000 °C were examined. Figure 3 shows the typical SEM and TEM images of samples G-PZ-1000-G and G-Z-1000-G, which were prepared with PZ and pure $ZnCl_2$ as the porogens, respectively. G-PZ-1000-G appeared to be composed of primary rough carbon particles with size around 10 nm, which were aggregated to give a porous and aerogel-like structure (Figure 3A, B). In contrast, G-Z-1000-G displayed larger particles with porous structure (Figure 3C, D). The differences in the morphology of G-PZ-1000-G and G-Z-1000-G suggest that the porogen played an important role in controlling the morphology of the resultant samples. The EDS profile (Figure 3E) of G-PZ-1000-G obtained during the TEM observation indicated the presence of the porogen salts, while in the XRD patterns of G-PZ-1000-G and G-Z-1000-G (Figure 3F) there was no obvious diffraction peaks ascribed to the porogen salts. These findings indicated that only trace amount of porogen salts was residual, and most of salts were removed via evaporation and followed washing. G-PZ-1000-G and G-Z-1000-G had similar XRD patterns with two diffraction peaks at $2\theta \approx 23°$ and $44°$ with large width and low intensity, which were ascribed to the graphitic carbon, albeit with disorder.[42]
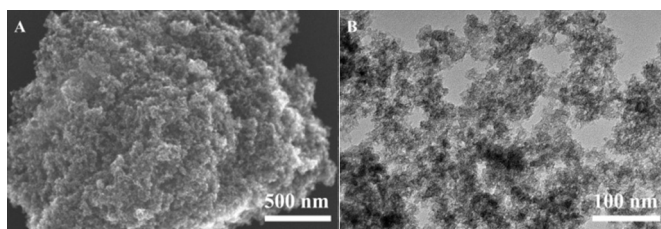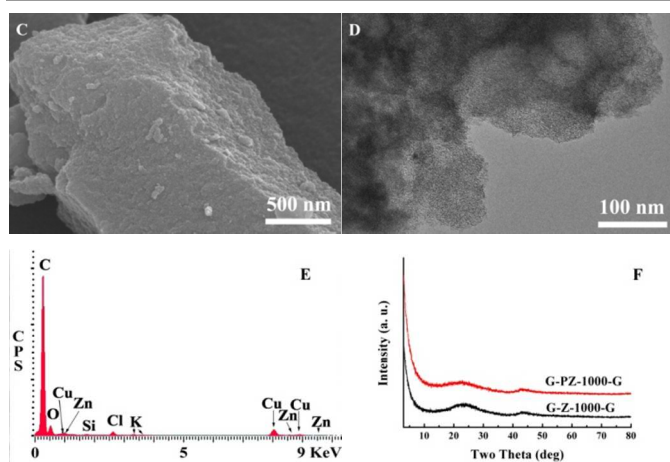
Figure 3 (A) SEM, (B) TEM images of G-PZ-1000-G; (C) SEM, (D) TEM images of G-Z-1000-G; (E) EDS profile of sample G-PZ-1000-G; (F) XRD patterns of sample G-PZ-1000-G and G-Z-1000-G.
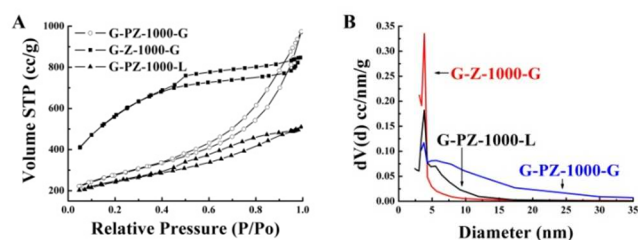

Figure 4 (A) Nitrogen sorption isotherms; (B) Pore size distribution of the samples.

Figure 4A shows N_2 sorption isotherms of the as-prepared carbon samples. G-PZ-1000-G exhibited a type IV isotherm with apparent hysteresis loop, an indication of mesopore structure. All the samples prepared in the presence of PZ (e.g., G-PZ-1000-L) displayed similar N_2 sorption isotherms to G-PZ-1000-G, suggesting that they had mesoporous structures. G-Z-1000-G also showed a type IV isotherm; however, it exhibited a relative higher N_2 adsorption in the low P/P_0 range compared to G-PZ-1000-L and G-PZ-1000-G, indicating the existence of mesopores together with plentiful micropores.

Based on the sorption isotherms, the BET SSA, pore volume, pore size and size distribution were obtained, and summarized in Table 1. G-PZ-1000-G showed a BET specific surface area (S_{total}) of 974 $m^2 \cdot g^{-1}$ and a pore volume (V_{total}) of 1.507 $cm^3 \cdot g^{-1}$ dominated with mesopore volume proportion of 91.6%. The V_{total} and mesopore volume proportion of this sample were much higher than those of G-PZ-1000-L and G-Z-1000-G prepared in this work and many other carbon-based materials such as N-doped porous carbon spheres,[30, 42, 43] and chemically activated mesoporous carbon.[23, 28, 44, 45] Compared to G-PZ-1000-G, G-PZ-1000-L obtained with a linear temperature program showed declined BET S_{total}, while G-Z-1000-G prepared using $ZnCl_2$ as porogen showed much higher BET S_{total}. These findings suggest that both heating way and porogen had important roles in controlling the BET S_{total}, V_{total}, mesopore volume proportion of the resultant carbons, and the conversion of glucose at 240 °C for 2 h was a crucial process for getting carbons with more mesopores.

Table 1 Pore textural property comparison of the as-prepared MCs[a] with those reported in literatures

Sample	S_{total} ($m^2 \cdot g^{-1}$)	Pore volume ($cm^3 \cdot g^{-1}$)			$V_{meso}/V_{total}(\%)$	Reference
		V_{total}	V_{micro}	V_{meso}		
G-PZ-1000-G	974	1.507	0.127	1.380	91.6	this work
G-PZ-1000-L	866	0.788	0.153	0.635	80.6	this work
G-Z-1000-G	2025	1.311	0.330	0.981	74.8	this work
G-Z-1000-L	1860	1.066	0.316	0.750	70.4	this work
S-800	1844	0.733	-	-	<18%	42
Bmp-dca_PZ_3_1000	2013	1.70	-	-	33.0	30
C-LiZn15/3	673	-	-	-	-	31
C-KOH-200	1148	1.000	-	-	66.0	23
ACD3	2841	1.692	-	-	50.2	28
S1-AZ-800	1721	0.971	-	-	<20%	45

[a] S_{total}: total BET specific surface area; V_{total}: total pore volume; V_{micro}: micropore volume; V_{meso}/V_{total}: mesopore volume proportion.

Figure 4B displays the pore size distribution of the above samples. An intense peak appeared at 3.0 nm in the pore size distribution plot of sample G-Z-1000-G, an indication of uniform pore size distribution, which may be ascribed to the role of $ZnCl_2$. In the plots of samples prepared using PZ as porogen, the peak at 3.0 nm was still present, accompanied with

a wider peak in the large pore size range. This indicated that in the PZ-mediated samples there appeared larger mesopores. One part pores had pore size around 3.0 nm, which may result from $ZnCl_2$ in PZ. The other mesopores with diameters larger than 3.0 nm may be caused by the synergistic effects of $ZnCl_2$ and KCl in PZ. From the pore size distribution plot of G-PZ-1000-

G, it was obvious that this sample had wide pore size distribution in the range from 3 to 30 nm, dominated with pore diameters larger than 3.0 nm. Compared to G-PZ-1000-G, G-PZ-1000-L had relatively narrow pore size distribution with pore diameters in the range of 3-15 nm. These results indicate that PZ was more favourable to the formation of large mesopores than $ZnCl_2$.

In order to explore the pore formation process, the samples prepared using a gradient temperature program at different final calcination temperatures were examined, and their pore textural properties are listed in Table 2. Sample G-PZ-240-L in brown colour showed a S_{total} of 973 $m^2 \cdot g^{-1}$, dominated with mesopores in proportion around 90%. The samples obtained via further calcining sample G-PZ-240-L using a heating rate of 1 °/min in the temperature range of 400-1000 °C (i.e., G-PZ-400-G, G-PZ-500-G, G-PZ-700-G and G-PZ-1000-G) displayed higher S_{total} around 1000 $m^2 \cdot g^{-1}$, probably ascribing to the further carbonization of the carbon materials. Samples G-PZ-400-G, G-PZ-500-G and G-PZ-700-G showed similar pore volumes and mesopore proportions, while G-PZ-1000-G showed the largest pore volume and mesopore proportion among these samples though its S_{total} was slightly lower. It was reported that $ZnCl_2$ could catalyze conversion of biomass derivatives via stripping away hydrogen and oxygen atoms in the carbon source as water rather than as hydrocarbons or as oxygenated organic compounds.[32] In this work, the eutectic salt PZ may have similar effect on glucose conversion, deduced from the TGA analysis for glucose and PZ mixture (Figure 1) and the FT-IR results analysis for carbon samples (Figure 2). All

samples underwent being preheated at 240 °C for 2 h. In this process, PZ was in molten state, and glucose was dissolved in PZ uniformly. PZ catalyzed the glucose conversion to the C=C and C=O containing compounds and further carbonization to form carbon materials rich in oxygen-containing groups. The phase separation of the newly formed carbons and PZ may lead to the formation of pores in carbons, dominated by mesopores. In the temperature range of 240-700 °C, increasing carbonization temperature mainly resulted in the removal of the oxygen-containing groups in the carbon materials, and the resultant samples (i.e., G-PZ-400-G, G-PZ-500-G, and G-PZ-700-G) showed the similar pore textural properties. Further increasing the temperature to 1000°C, the micropores may be destroyed by collapsing or merging into mesopores, leading to an increase in total pore volume and mesopore volume proportion.

It was reported that the amount of porogen was an important factor to influence the textural properties of the resultant carbon materials.[30] In this work, two other samples were prepared with the ratios of glucose to porogen at 1: 1 and 1: 6, respectively. Compared to G-PZ-1000-G, the samples obtained with the ratio of glucose to porogen at 1: 1 and 1: 6 displayed comparable S_{total}. Interestingly, the pore volumes and mesopore proportions of the carbons increased with the amount of PZ used. Especially, the sample obtained with the ratio of glucose to porogen at 1: 6 showed a pore volume of 2.727 $cm^3 \cdot g^{-1}$ and mesopore proportion of 92.2%, much higher than those reported.[22, 25, 30, 35]

Table 2 Pore textural properties of the mesoporous carbon materials from glucose

Sample name	S_{total} ($m^2 \cdot g^{-1}$)	Pore volume ($cm^3 \cdot g^{-1}$)			V_{meso}/V_{total} (%)
		V_{total}	V_{micro}	V_{meso}	
G-PZ-240-L	793	1.266	0.122	1.144	90.4
G-PZ-400-G	1104	1.386	0.213	1.173	84.6
G-PZ-500-G	1017	1.307	0.209	1.098	84.0
G-PZ-700-G	999	1.299	0.208	1.091	84.0
G-PZ-1000-G	974	1.507	0.127	1.380	91.6
[a]G-PZ-1000-G	1116	0.786	0.262	0.524	66.7
[b]G-PZ-1000-G	1297	2.727	0.214	2.513	92.2

[a] The ratio of glucose/eutectic salt PZ = 1: 1. [b] The ratio of glucose/eutectic salt PZ = 1: 6.

Based on the above results, cellulose and lignin instead of glucose were used as the carbon resources for the preparation of mesoporous carbon materials using the similar procedures with a ratio of carbon resource to PZ at 1: 3, and the resultant samples are listed in Table 3. The results showed that the porogen salt PZ had a similar effect on the carbon materials derived from cellulose and lignin. All samples derived from cellulose showed porous structures with surface area higher than 1200 $m^2 \cdot g^{-1}$. Samples M-PZ-400-G and M-PZ-700-G had similar mesopore proportion and pore volume, while sample M-

PZ-1000-G showed higher pore volume and mesopore proportion. These phenomena were similar to those observed in the cases of glucose used as the carbon source. Notably, the sample derived from lignin, L-PZ-1000-G, also showed high surface area, 1066 $m^2 \cdot g^{-1}$, while its pore volume and mesopore proportion decreased obviously compared to the samples obtained from glucose and cellulose, which may be related to the aromatic structures. In addition, the yields of all the samples carbonized at 1000 °C were about 20 wt%.

Table 3 Pore textural properties of the mesoporous carbon materials from cellulose and lignin

Sample	S_{total} (m^2·g^{-1})	Pore volume (cm^3·g^{-1})			V_{meso}/V_{total} (%)
		V_{total}	V_{micro}	V_{meso}	
M-PZ-400-G	1261	1.013	0.236	0.777	76.7
M-PZ-700-G	1224	1.014	0.227	0.787	77.6
M-PZ-1000-G	1244	1.123	0.140	0.983	87.5
L-PZ-1000-G	1066	0.730	0.269	0.461	63.2

The resultant highly mesoporous carbons are expected to have good performances for different applications. In this work, sample G-PZ-1000-G was used as a support to immobilize palladium nanoparticles, resulting in a Pd/G-PZ-1000-G nanocomposite with Pd loading of 5 wt%. The TEM image and particle size distribution of this composite are shown in Figure 5. It is clear that the Pd nanoparticles were uniformly distributed on the support, and the average particle size was centered about 1.2 nm. Pd/G-PZ-1000-G was applied in the hydrogenation of styrene in n-heptane at 30 °C and 1 MPa H$_2$ pressure, which displayed high performance for this reaction with a turnover frequency (TOF) (mole of converted styrene per molar Pd per hour) of 15500 h^{-1}, much better than that of a commercial Pd/C (5 wt%) catalyst with a TOF of 8900 h^{-1} under the same reaction conditions.
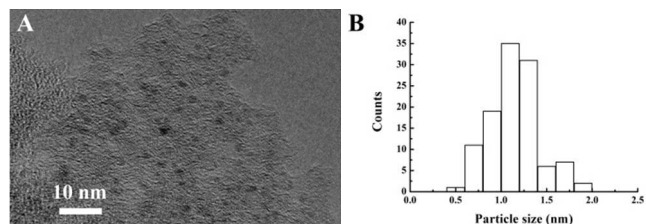

Figure 5 (A) TEM image of Pd/G-PZ-1000-G; (B) Particle size distribution obtained by counting over 100 particles.

Conclusions

Highly mesoporous carbons were prepared via carbonization of biomass feedstocks (including glucose, cellulose and lignin) with eutectic salt (KCl/ZnCl$_2$, PZ) as the porogen. PZ played the crucial role in the formation of mesopores in the resultant carbons, and a series of MCs with high mesopore proportion were obtained. Especially, the MC derived from glucose via a gradient temperature program and glucose to PZ ratio of 1: 6 showed a mesopore proportion of 92.2% and a BET SSA up to 1297 m^2·g^{-1}. This work offers a simple way to prepare MCs from biomass, and the resultant MCs may have promising applications in catalyst support, separation sorbent and electrode material.

Acknowledgements

Notes and references

Institute of Chemistry, Chinese Academy of Sciences No. 2, Zhongguancun Beiyijie, Beijing 100190 (China)
E-mail: liuzm@iccas.ac.cn

1. J. R. Holst and A. I. Cooper, *Adv Mater*, 2010, **22**, 5212-5216.
2. J. Lee, S. Yoon, T. Hyeon, S. M. Oh and K. B. Kim, *Chem. Commun.*, 1999, 2177-2178.
3. T. Harada, S. Ikeda, M. Miyazaki, T. Sakata, H. Mori and M. Matsumura, *J. Mol. Catal. A Chem.*, 2007, **268**, 59-64.
4. D. Lee, J. Lee, J. Kim, J. Kim, H. B. Na, B. Kim, C. H. Shin, J. H. Kwak, A. Dohnalkova, J. W. Grate, T. Hyeon and H. S. Kim, *Adv. Mater.*, 2005, **17**, 2828-2833.
5. A. Vinu, C. Streb, V. Murugesan and M. Hartmann, *J. Phys. Chem. B*, 2003, **107**, 8297-8299.
6. D. Saha and S. Deng, *J. Collid Interf. Sci.*, 2010, **345**, 402-409.
7. C. Liang, Z. Li and S. Dai, *Angew. Chem. Int. Ed. Engl.*, 2008, **47**, 3696-3717.
8. B. Tiryaki, E. Yagmur, A. Banford and Z. Aktas, *J. Anal. Appl. Pyrolysis*, 2014, **105**, 276-283.
9. E. Yagmur, M. S. Tunc, A. Banford and Z. Aktas, *J. Anal. Appl. Pyrolysis*, 2013, **104**, 470-478.
10. E. Yagmur, M. Ozmak and Z. Aktas, *Fuel*, 2008, **87**, 3278-3285.
11. N. V. Sych, S. I. Trofymenko, O. I. Poddubnaya, M. M. Tsyba, V. I. Sapsay, D. O. Klymchuk and A. M. Puziy, *Appl. Surf. Sci.*, 2012, **261**, 75-82.
12. J. Wang, A. Heerwig, M. R. Lohe, M. Oschatz, L. Borchardt and S. Kaskel, *J. Mater. Chem.*, 2012, **22**, 13911.
13. I. I. Gurten, M. Ozmak, E. Yagmur and Z. Aktas, *Biomass and Bioenergy*, 2012, **37**, 73-81.
14. J. Yang and K. Qiu, *Chem. Eng. J.*, 2011, **167**, 148-154.
15. H. S. Teng and T. S. Yeh, *Ind. Eng. Chem. Res.*, 1998, **37**, 58-65.
16. M. Sevilla, A. B. Fuertes and R. Mokaya, *Energy Environ. Sci.*, 2011, **4**, 1400.
17. D. Kalderis, S. Bethanis, P. Paraskeva and E. Diamadopoulos, *Bioresour. Technol.*, 2008, **99**, 6809-6816.
18. K. N. M. André Pinkert, Shusheng Pang and Mark P. Staiger, *Chem. Rev.*, 2009, **109**, 6712-6728.

19. P. Maki-Arvela, T. Salmi, B. Holmbom, S. Willfor and D. Y. Murzin, *Chem. Rev.*, 2011, **111**, 5638-5666.

20. G. W. Huber, S. Iborra and A. Corma, *Chem. Rev.*, 2006, **106**, 4044-4098.

21. V. S. Nevin Yalçın, *Carbon*, 2000, **38**, 1943.

22. T.-P. Fellinger, R. J. White, M.-M. Titirici and M. Antonietti, *Adv. Funct. Mater.*, 2012, **22**, 3254-3260.

23. D. Saha, Y. Li, Z. Bi, J. Chen, J. K. Keum, D. K. Hensley, H. A. Grappe, H. M. Meyer, 3rd, S. Dai, M. P. Paranthaman and A. K. Naskar, *Langmuir*, 2014, **30**, 900-910.

24. M. Antonietti, N. Fechler and T.-P. Fellinger, *Chem. Mater.*, 2014, **26**, 196-210.

25. V. Gómez-Serrano, E. M. Cuerda-Correa, M. C. Fernández-González, M. F. Alexandre-Franco and A. Macías-García, *Mater. Lett.*, 2005, **59**, 846-853.

26. B. Cardoso, A. S. Mestre, A. P. Carvalho and J. Pires, *Ind. Eng. Chem. Res.*, 2008, **47**, 5841-5846.

27. Q. G. a. J. H. Huanlei Wang, *J. Am. Chem. Soc.*, 2009, **131**, 7016-7022.

28. X. Song, Y. Zhang and C. Chang, *Ind. Eng. Chem. Res.*, 2012, **51**, 15075-15081.

29. Y. Xiao, H. Chen, M. Zheng, H. Dong, B. Lei and Y. Liu, *Mater. Lett.*, 2014, **116**, 185-187.

30. N. Fechler, T. P. Fellinger and M. Antonietti, *Adv. Mater.*, 2013, **25**, 75-79.

31. N. Fechler, S.-A. Wohlgemuth, P. Jäker and M. Antonietti, *J. Mater. Chem. A*, 2013, **1**, 9418-9421.

32. Z. H. Hu, M. P. Srinivasan and Y. M. Ni, *Carbon*, 2001, **39**, 877-886.

33. W. T. Tsai, C. Y. Chang and S. L. Lee, *Bioresour. Technol.*, 1998, **64**, 211-217.

34. M. Z. Hussein, R. S. H. Tarmizi, Z. Zainal, R. Ibrahim and M. Badri, *Carbon*, 1996, **34**, 1447-1449.

35. A. Ahmadpour and D. D. Do, *Carbon*, 1997, **35**, 1723-1732.

36. E. GonzalezSerrano, T. Cordero, J. RodriguezMirasol and J. J. Rodriguez, *Ind. Eng. Chem. Res.*, 1997, **36**, 4832-4838.

37. D. Saha, E. A. Payzant, A. S. Kumbhar and A. K. Naskar, *ACS Appl. Mater. Interfaces*, 2013, **5**, 5868-5874.

38. X. Liu, N. Fechler and M. Antonietti, *Chem. Soc. Rev.*, 2013, **42**, 8237-8265.

39. X. Liu and M. Antonietti, *Carbon*, 2014, **69**, 460-466.

40. X. Liu, C. Giordano and M. Antonietti, *Small*, 2014, **10**, 193-200.

41. M.-M. Titirici, R. J. White, C. Falco and M. Sevilla, *Energy Environ. Sci.*, 2012, **5**, 6796-6822.

42. S. Gao, Y. Chen, H. Fan, X. Wei, C. Hu, H. Luo and L. Qu, *J. Mater. Chem. A*, 2014, **2**, 3317-3324.

43. X. Wang, J. S. Lee, C. Tsouris, D. W. DePaoli and S. Dai, *J. Mater. Chem.*, 2010, **20**, 4602-4608.

44. H. Deng, L. Yang, G. Tao and J. Dai, *J. Hazard. Mater.*, 2009, **166**, 1514-1521.

45. S. Gao, H. Fan, Y. Chen, L. Li, Y. Bando and D. Golberg, *Nano Energy*, 2013, **2**, 1261-1270.

Graphic Abstract

Highly mesoporous carbons (MCs) derived from biomass feed stocks were prepared using eutectic salt (KCl/ZnCl$_2$) as the porogen agent and catalyst through gradient heating program.